Journal of Hydrology: Regional Studies 37 (2021) 100880

Contents lists available at ScienceDirect

Journal of Hydrology: Regional Studies

journal homepage: www.elsevier.com/locate/ejrh

Climate change and water abstraction impacts on the long-term variability of water levels in Lake Bracciano (Central Italy): A Random Forest approach

N. Guyennon [a,*], F. Salerno [b], D. Rossi [a], M. Rainaldi [c], E. Calizza [d], E. Romano [a]

[a] National Research Council, Water Research Institute, IRSA-CNR, Roma, Italy
[b] National Research Council, Water Research Institute, IRSA-CNR, Brugherio, Italy
[c] Ministry of Education, University and Research Viale Trastevere, 76/a – 00153, Roma, Italy
[d] Department of Environmental Biology, Sapienza University of Rome, via dei Sardi 70, 00185, Rome, Italy

ARTICLE INFO

Keywords:
Machine learning
Random forest
Lake bracciano
Climate change
Water abstraction
Water management

ABSTRACT

Study Region: Lake Bracciano has been historically used as a strategic water reservoir for the city of Rome (Italy) since ancient times. However, following the severe water crisis of 2017, water abstraction has been completely stopped.
Study Focus: The relative impact of the various drivers of change (climatological and management) on fluctuations in lake water level is not yet clear. To quantify this impact, we applied the Random Forest (RF) machine learning approach, taking advantage of a century of observations.
New Hydrological Insights for the Region: Since the late 1990s the monthly variation in lake water levels has doubled, as has variation in monthly abstraction. Increased variation in annual cumulated precipitation and a rise in mean air temperature have also been observed. The RF machine learning approach made it possible to confirm the marginal role of temperature, the increasing role of abstraction during the last two decades (from 24 % to 39 %), and the key role played by the increased precipitation variability. These results highlight the notable prediction and inference capabilities of RF in a complex and partially unknown hydrological context. We conclude by discussing the limits of this approach, which are mainly associated with its capacity to generates scenarios compared to physical based models.

1. Introduction

As a consequence of its proximity to the city of Rome (only 37 km), Lake Bracciano (with a surface area of 57.6 km^2) has historically been used as a strategic water reservoir since Roman Times, when it was also widely used for fishing and recreational purposes as demonstrated by numerous paintings in nearby Roman villas (Cordiano et al., 2014). The natural hydrology of Bracciano Lake remained unchanged until the 17th century, when under Pope Paolo V, a dam was built on the Arrone River, the natural lake outflow, in order to extract water for human consumption and controlling the lake's water level (L) in case of floods. The 1920s saw the start of abstraction by means of hydraulic pumps, leading to greater variability of L. Since 1909, water abstraction from the lake has been managed by the ACEA water utility. Abstraction has varied significantly over the years, ranging from 0 to more than 2 $m^3 s^{-1}$. After the water crises affecting Central Italy in 2017,which severely impacted Lake Bracciano (Rossi et al., 2019), abstraction is currently

* Corresponding author.
E-mail address: guyennon@irsa.cnr.it (N. Guyennon).

https://doi.org/10.1016/j.ejrh.2021.100880
Received 14 April 2021; Received in revised form 1 July 2021; Accepted 24 July 2021
Available online 17 August 2021

interrupted and the lake is considered an "emergency resource" to be used only in the event of significant water scarcity (ACEA, 2015). Low *L* was recorded in 1955, 1990, 2003 and 2008, but the absolute minimum was recorded in 2017 (−198 cm). As a consequence, serious management concerns have been raised in recent years.

Currently, the relative impact of the various drivers of change (climate and management) on the lake water level fluctuations is still not clear. As presented in details in § 2.1, it is known that the water budget of Lake Bracciano is driven by both surface and sub-surface flows, although the relative contribution of these components is not clear (Taviani and Henriksen, 2015).

Regarding the quantitative management of the resource, a sound knowledge of the lake water budget, as well as its temporal hydrogeological dynamics, is fundamental for developing effective policies over a range of time scales. On the one hand the Lake Bracciano is currently considered an "emergency resource", to be used only in the event of failure of the main resources supplying the city of Rome under ordinary conditions, and therefore the impact of a sudden and intense abstraction must be carefully evaluated. On the other hand, exploitation of the lake over longer periods (years) needs to take account of the normal fluctuation of the water level due to multi-years or decadal oscillations in precipitation (Romano and Preziosi, 2013), which is possibly affected by climate change (Armenia et al., 2019).

Considering the qualitative aspects, water level fluctuations can strongly impact the lake ecosystem and, consequently, ecosystem services provided to the local economy (Galloway et al., 2003; Kendall et al., 2010; Calizza et al., 2021). Previous studies show in the last 20 years major alterations to lake ecosystem functioning, such as the near or complete disappearance of littoral habitats and the reduction by several tens of hectares of deep-water plant communities such as charophytes (Carpenter and Lodge, 1986; Azzella, 2014; Azzella et al., 2017). The direct consequence of large fluctuations in water levels was the eutrophication of the banks, with consequent invasion of the riparian communities by alien species and the alteration of the fauna in terms of both vertebrate species and riparian and aquatic invertebrates (Azzella, 2014; Baccetti et al., 2017). *L* fluctuations generally impact the riparian vegetation, with a consequent damage to lake self-purification processes, fundamental for maintaining water quality as a resource for human consumption, but also for maintaining appropriate habitats for biodiversity conservation (Ostroumov, 2017; Calizza et al., 2021). As an example, two recent studies from the lake (Costantini et al., 2018; Calizza et al., 2021) demonstrated that the loss of riparian and submerged vegetation in the proximity of the lake shore made lake fish communities vulnerable to the invasion by a bass species (*Micropterus salmoides*), leading to reduced fish diversity and altered food web structure. Calizza et al. (2021) found that 100 linear meters of highly vegetated lake shores reduced the economic impact of the invader on the two most commercially valuable fish species by approximately 1400 € per year in comparison to poorly vegetated areas. This suggests that water level reduction, which mainly impacts lake littoral areas, has potentially detrimental effects on multiple ecosystem services provided by the lake ecosystem.

This study aims to describe the long term variability of the Lake Bracciano levels as a function of climate (temperature and precipitation regime) and abstraction management. The most straightforward and common way to perform this analysis is to describe the processes driving the surface and subsurface flows by means of suitable physical parameter-based equations (basically, mass and energy conservation equations). However, this approach needs to take into account of a large number of space and time scales, which in turn implies the adoption of appropriate equations, posing the consequent question of the most suitable scales for parameterization (Blöschl, 2001; Sivapalan, 2003). Therefore, in order to adequately describe the hydrology (and possibly the hydrogeology) of a given catchment area, it is necessary to have not only a large number of observations, but also consistency of space and time data, as well as the scales of the adopted physically-based equations. For this reasons, to overcome the issues arising from a multi-scale physical description, in the last decade the use of statistical learning approaches has significantly increased (Ardabili et al., 2019). Generally, these procedures detect and describe statistical patterns in univariate or multivariate datasets regardless of the underlying physical processes. Among the recent techniques developed and applied for hydrological contexts, we shall cite Artificial Neural Networks (e.g., Dawson and Wilby, 2001; Bowden et al., 2005; Abrahart et al., 2012), Bayesian Network (Aguilera et al., 2011; Phan et al., 2016), Support Vector Machine (i.e., Raghavendra and Deka, 2014) and Random Forest (Breiman, 2001; Naghibi et al., 2019; Tyralis et al., 2019).

According to James et al. (2013), among these machine learning algorithms, RF is considered the most interpretable non-parametric approach (whereas, Support Vector Machine is considered the most interpretable of the parametric techniques).

Furthermore, the Random Forest (*RF*) technique has been recognized to be effective at capturing the non-linear dependency of predictors and dependent variables (Boulesteix et al., 2012). In addition, Random Forest makes it possible to assess the relative significance of predictor variables, by means of variable importance metrics (Ziegler and König, 2014; Díaz-Uriarte and De Andres, 2006). This feature is particularly attractive in the Lake Bracciano case-study, where, as explained in details in Section 2, there is insufficient data to determine a reliable water budget (i.e., there is a lack of groundwater flow data), thus making it impossible to distinguish between the relative impacts of distinct forcing factors on the variability of *L*.

In this study, the capability of the *RF* machine learning approach to estimate the relative impact of climate and management on Lake Bracciano water levels is tested. The results will be analyzed with reference to the potential of the adopted technique in hydrological contexts, especially when observations are missing, pointing out implications on future management of water abstraction.

2. Case study

Lake Bracciano is an oligo-mesotrophic (Rossi et al., 2010; Costantini et al., 2018) sub-circular volcanic lake located 32 km Northwest of Rome (Latium, Italy). This last became active 0.6 Ma and was characterized by explosive eruptions causing the deposition of pyroclastic flows and falls (e.g. Nicolosi et al., 2019). The lake belongs to the Sabatino Volcanic District, which is one of the Roman magmatic Province District developed during Pleistocene times due to the extensional tectonics that led to the Tyrrhenian Sea opening (Malinverno and Ryan, 1986). During this extensional tectonic phase, the carbonate substratum was displaced in NW-SE and NE-SW

trending horst and graben structures (Di Filippo et al., 1998; De Rita et al., 1996), which allowed a depression today filled by lake Bracciano.

Lake Bracciano has a surface area of 57.6 km^2, a total volume of $5.13 \cdot 10^9$ m^3 and a circular perimeter of 31.981 km (Rossi et al., 2019), with a maximum depth of 165 m (Fig. 1). It has an elevation of 163.04 m a.s.l. (altitude of the River Arrone emissary, here considered as the hydrometric zero of the lake), defined as the reference level (Fig. 1). The lake's catchment area measures 147.483 km^2, the hydrographic network consisting of several small inflows (Fig. 1). The high percentage of the hydrological and hydrogeological basins covered by the lake itself (about 30 %) makes lake Bracciano particularly sensitive to climatic variations (Taviani and Henriksen, 2015; Rossi et al., 2019).

2.1. Hydrology

The lake water balance on a monthly scale can be expressed as:

$$\Delta V_i = V_i - V_{i-1} = P_i - E_i - Q_{out\,i} + R_i + Q_i^{GW_{in}} - Q_i^{GW_{out}} \quad (1)$$

where V_i and V_{i-1} are the lake volumes at month i and i-1, respectively; P_i is precipitation over the lake; E_i is evaporation from the lake surface; $Q_{out\,i}$ is abstraction from the lake; R_i is runoff to the lake; $Q_i^{GW_{in}}$ and $Q_i^{GW_{out}}$ are groundwater inflow and outflow respectively.

Some components of the water budget can be directly measured or estimated on the basis of other observed variables, while other terms are missing due to the lack of data. Specifically, V_i and V_{i-1} are calculated from the observed L and the lake's hypsographic curve (§2.2.4); P_i is recorded with an automatic weather station (§ 2.2.1); E_i is estimated by means of the Penman-Monteith equation from

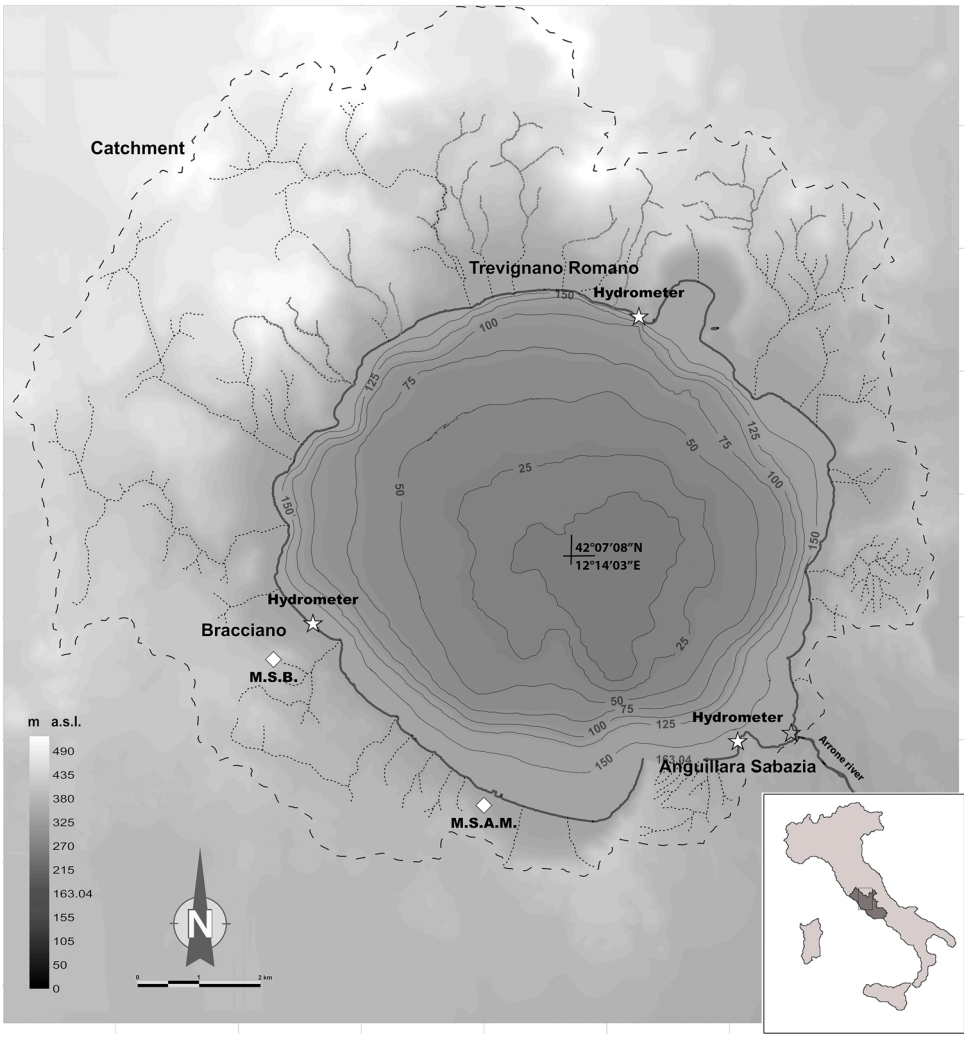

Fig. 1. Elevation map of Bracciano Lake. Watershed (dashed line), streams (dotted lines), shore line (black line, at reference level), lake isobaths (thin black lines, m a.s.l.), hydrometers (stars), Bracciano Weather Station, Aereonautica Militare Weather Station.

automatic weather station and reanalysis data (§2.2.2 and §2.2.3); $Q_{out\,i}$ is provided by the resource manager (ACEA ATO2) (§2.2.4). Neither $Q_i^{GW_{in}}$ nor $Q_i^{GW_{out}}$ are not available for this case study, due to the lack of continuous measurements of piezometric heads and neither is the surface runoff (R_i is not measured, due to the distinctive hydrographic network, which does not have any main tributary suitable for installing automatic hydrometers).

The lack of these input data prevents the use of a classic modelling approach in order to estimate the lake water budget. It is important to stress that previous models (Taviani and Henriksen, 2015) aimed at simulating the lake water budget in transient conditions were calibrated with reference to a set of piezometric measurements taken on a single occasion in 2009, and thus did not provide a robust estimate of the hydrodynamics parameters of the aquifer (for either its inflow or outflow component). In fact, the use of a single set of data to calibrate the model in transient conditions necessarily results in the non-uniqueness of the calibration procedure. Therefore, the dynamics of the groundwater and surface runoff components are unknown. This lack of data does not allow for the adoption of a modelling approach that would produce a sound estimate of the lake water budget.

2.2. Dataset

2.2.1. Precipitation

The monthly cumulated precipitation for the 1955–2019 period was measured at the "Aeronautica Militare di Vigna di Valle" weather station (WS) (Fig. 1), managed by Servizio Meteorologico Aeronautica Militare (www.meteoam.it), for the 1944–1955 period, data were collected at the Bracciano WS by the Lazio Regional Administration (3.8 km from the Aeronautica Militare Vigna di Valle WS, Fig. 1); and for 1921–1944 period, data were collected by ISPRA (www.isprambiente.gov.it) at the Aeronautica Militare di Vigna di Valle WS. In order to ensure the homogeneity of the precipitation data, the monthly cumulated precipitation time series from the Bracciano WS was statistically downscaled to that of the Aeronautica Militare di Vigna di Valle WS, which was used as a reference in accordance with a monthly quantile mapping procedure (Guyennon et al., 2013), considering 812 common observations during the 1940–2018 period. Hereinafter, the resulting monthly cumulated precipitation time series from 1921 to 2019 will be referred to as P (Fig. 2a).

2.2.2. Temperature

This study use minimum and maximum daily temperature data recorded at the Aeronautica Militare di Vigna di Valle WS during the 1955–2019 period (Fig. 1). Previous data were considered unsuitable due to their fragmentation. Hereinafter, the monthly mean of daily mean temperature will be referred to as T (Fig. 2b).

2.2.3. Other meteorological data

Surface evaporation from the lake was estimated using the daily minimum, mean and maximum temperature, wind speed, relative humidity and atmospheric pressure measured at the Aeronautica Militare di Vigna di Valle WS for the 2007–2017 period, as well as the daily incoming solar radiation obtained from ERA interim reanalysis (Dee et al., 2011).

2.2.4. Abstraction

Monthly abstraction from the lake (Fig. 2c) has been supplied by the ACEA-ATO2 for 1975–2020 period, while previous abstraction was assumed constant (1 $m^3\ s^{-1}$) (ACEA-ATO2, personal communication). Hereinafter, the monthly mean of daily mean temperature will be referred as Q_{out} (Fig. 2b).

2.2.5. Lake level variations

The lake water levels (Fig. 2 d) were measured at three hydrometer stations (Bracciano, Anguillara and Trevignano Romano) installed by the Bracciano-Martignano Park Authority (Fig. 1). Hereinafter, the monthly lake levels will be referred to as L (Fig. 2d).

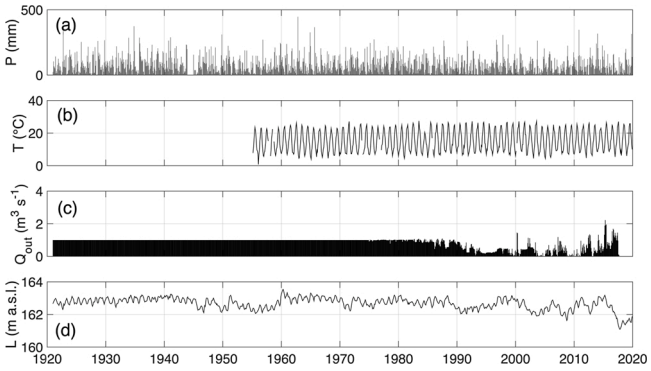

Fig. 2. a) Monthly cumulated precipitation P (mm), b) mean air temperature T (°C), c) water abstraction Q_{out} ($m^3\ s^{-1}$), and d) lake levels L (m a. s.l.).

3. Methods

The relative impacts of the potential drivers of change (cliamte and management) on the lake levels on short (seasonal) and long (over the 100 years) time scales were investigated as follows:

- The precipitation regime was analyzed by means of the Standardized Precipitation Index (SPI) (McKee et al. 1993) computed at various time scales, coupled with analysis of the linear correlation analysis between precipitation regime and variations in L (§ 3.1).
- The long-term relationships between precipitation and L was further investigated by means of Sen's slope method (Sen, 1968) and the cross-wavelet analysis (Grinsted et al., 2004) (§ 3.2).
- The possible impact of long-term variations in lake evaporation, due to the temperature increase observed during the 1955–2019 period was estimated using the Penman equation (§ 3.3).
- Finally, the relative impacts of meteorological forcing and abstraction pressures were explored by means of a machine learning technique, i.e. Random Forest (§ 3.4).

3.1. Standardized precipitation index

The Standardized Precipitation Index (SPI, McKee et al., 1993, 1995) recommended by the World Meteorological Organization (WMO, 2012), is widely used to represent the anomalies of cumulated precipitation over an assigned time scale (usually from 1 to 24 months) with respect to standard conditions (i.e., the long-term average over a given baseline). The SPI is computed by fitting the observed cumulative distribution function by means of a gamma distribution and inverting the fitted function on a normal distribution. Following the approach adopted by Nalbantis and Tsakiris (2009), who used an SPI linear function to compute hydrological indexes, multilinear regressions of SPIs computed over different time scales can be used to represent hydrogeological processes (e.g., springs discharges, Romano et al., 2013) and hydrological processes (e.g., surface runoff, Guyennon et al., 2016; Romano et al., 2017, 2018). The different precipitation time scales (in this work from SPI1 to SPI24, the number indicating the time scale in month) are representative of different hydrological processes: clearly, short time scales reflect rapid responses of the catchment area (run off), whereas longer time scales (up to 24 months) represent slower dynamics, such as the groundwater flow. Analysis of the relationship between the SPIs estimated for a range of time scales and the monthly variations in lake Bracciano *L* makes it possible to account for the various hydrological and hydrogeological processes affecting the oscillation of the lake level.

3.2. Trends and long-term variability

We used Sen's slope, proposed by Sen (1968), as a robust linear regression allowing the quantification of the potential linear trends in the time series. The Mann-Kendall (MK) test (Kendall, 1948) was used to test the alternative hypothesis that the data follow a monotonic trend (e.g. Guyennon et al., 2017; Thakuri et al., 2019). The observed change in long-term variability was estimated as the standard deviation of monthly time series of each considered variable based on 10-years moving windows. The time series of the frequency content of common oscillations across the time scales were investigated by means of cross wavelet analysis. The latter was performed in this study using a free Matlab-software package proposed by Grinsted et al. (2004), corrected from the bias in the wavelet power spectrum by adopting a physically consistent definition of energy for the wavelet power spectrum following Liu et al. (2007). Following Guyennon et al. (2014), we defined the global cross wavelet spectrum (GXWS), for both amplitude and phase, as the time integration of the respective coefficients within the 95 % confidence interval and a cone of influence. This adjusted wavelet power spectrum allowed comparison of global spectral peaks across time scales.

3.3. Open water surface evaporation

Penman's combined heat balance and aerodynamic equation (Penman, 1948,1956; Romano and Giudici, 2007, 2009) was used to estimate evaporation from the open water surface of lake Bracciano for the period 2007–2017, using the modified wind function adopted by Linacre (1993). Short wave reflectivity and the emissivity coefficients of the water surface, as well as longwave radiation coefficients for clear skies, were estimated following Shuttleworth (1993). To estimate possible long-term variations in open water evaporation, a mean variation of 2 °C [-1 + 1] in air temperature compared to the mean value of the 2007–2017 period was considered. The other meteorological parameters that are required in order to compute evaporation via the Penman equation (i.e., wind speed, relative humidity, atmospheric pressure and downward solar radiation) were kept unchanged.

3.4. Random forest

Random Forest (*RF*), among the ensemble machine learning methods, is a bagging (bootstrap aggregating) method that generates a large numer of regression trees (Loh, 2011) that are independently constructed using a bootstrap sample of the dataset (Breiman, 2001; Liaw and Wiener, 2002). A regression tree splits the predictor space into non-overlapping regions. In the following, the points along the tree where the predictor space is split are referred to as *nodes* and terminal nodes are referred to as *leaf*. An ensemble of trees is referred to as a *forest*. Random forest differs from previous bagging methods (Breiman, 1996) because the regression tree is not only based on a different dataset, but also constructed differently through a further random selection of predictors applied at each node. The purpose of

these two sources of randomness is to decrease the variance of the forest estimator. An extensive review of the theoretical aspects of *RF* can be found in Biau and Scornet (2016). *RF* performs very well compared to many other classifiers, including discriminant analysis, support vector machines and neural networks, and is robust against overfitting (Breiman, 2001). All *RF* results presented below were run using Scikit-learn, a Python module integrating a wide range of state-of-the-art machine learning tools (Pedregosa et al., 2011; Buitinck et al., 2013).

3.4.1. Hyperparameter tuning

While model parameters are learned during the training phase, hyperparameters must be set before the training. The *RF* hyperparameters include, among others, the number of decision trees in the forest and the number of features (or variables) considered by each tree when splitting a node. Hyperparameter tuning is obtained by means of a "trial-and-error" procedure, evaluating *a posteriori* the performance of each model. However, evaluating each model on the basis of training set alone can lead to overfitting. Therefore, the hyperparameter optimization involves 5-fold cross-validation, conducting an exhaustive search over specified parameter values for an estimator (using GridSearchCV from Scikit-learn) in accordance with Paper (2020). The hyperparameters considered in this study are shown in Table 1.

3.4.2. Learning and testing data set

For each forest (ensemble of regression trees), the overall dataset was randomly split into learning and testing datasets, each built with half of the overall available data. Moreover, a stratified sampling was applied to the predictand, so that each forest uses a learning data set representative of the predictand distribution.

3.4.3. Variable importance

In *RF* application, "feature importance" or "variable importance" is used to identify, for each forest, the relative weight of each variable in estimating the variation in *L*. We calculated the drop-column importance of each predictand following Strobl et al. (2008) and Parr et al. (2018). The drop-column importance of a predictand is computed by comparing the error in a trained *RF* model to a retrained version of the model from which the feature has been omitted. This offers a direct and robust, although computationally expensive, method for calculating the relative importance of variables. It is worth stressing that the method does not normalize the importance values (i.e., the weight of each variable in the prediction). The latter can be achieved by dividing the raw importance by its standard error. However, raw importance has better statistical properties (Strobl and Zeileis, 2008; Díaz-Uriarte and De Andres, 2006). As we are interested in the relative predictive importance of the variable, we consider the unscaled values.

4. Results

Fig. 3a presents the seasonal, annual and bi-annual precipitation anomalies as estimated by the SPI calculated for precipitation cumulated over 6, 12 and 24 months, together with *L* (Fig. 3a, right axis). Most of the variability of *L* is driven by the long-term precipitation anomalies. Indeed, the maximum Pearson's correlation coefficient between *L* and SPI over the past century (0.71) is seen at SPI24 (Fig. 3b). In contrast, the correlation reached its lowest value for short-term variation (SPIs of a few months). The behaviour of the correlation coefficients suggests that the short-term hydrological components such as direct precipitation on the lake and runoff impact *L* only slightly, while a greater role is played by slow hydrological dynamics, most probably the groundwater flows.

Concerning long-term trends, Sen's slope applied to the *L* time series indicates a statistically significant downward trend for the 1921–2019 period (-0.43 cm y^{-1}, $p < 0.01$). Fig. 3a suggests that this decrease can be mainly attributed to the long-term decrease in precipitation (-1.7 mm y^{-1}, $p < 0.05$ over the same period) possibly resulting in a decrease in groundwater recharge.

To better explore the relationship between the slow oscillations in precipitation and the related oscillations in the lake water level, a Cross Wavelet Analysis between *L* and SPI24 was conducted. This analysis, presented in Fig. 3c, shows a continuous common oscillation at the annual scale and a strong in-phase intermittent common oscillation at a pluri-annual scale ranging from 3 to 5 years (centered on 4.5 year, Fig. 3d). These large long-term common oscillations clearly increase during the last two decades, although they can also be observed from mid 1940s to the early 1960s and during the early 1970s, but for shorter periods and at lower intensity. These results suggest that the recent collapse of *L* may be driven by an increased in the amplitude of long-term precipitation oscillations, rather than by a simple linear decrease in precipitation.

Variation not attributable to SPI24 may be due to (i) the response to variation in precipitation on shorter time scales (represented by

Table 1
List of Random Forest hyperparameters considered in this study.

Hyper-parameter	Short description	Range tested
Number of estimators	Number of regression trees to be implemented	10, 50, 100, 200
Maximum features	Maximum number of features/variable to be considered for splitting a node	All, square root of number of feature, log2 of number of feature
Minimum samples split	Minimum number of samples required to split a node	2, 4, 816
Minimum sample leaf	Minimum number of samples required to be at leaf node.	1,2,4,816
Minimisation criterion	The function for measuring the quality of a split.	Root Mean Squared Error (RMSE), Mean absolute Error (MAE)

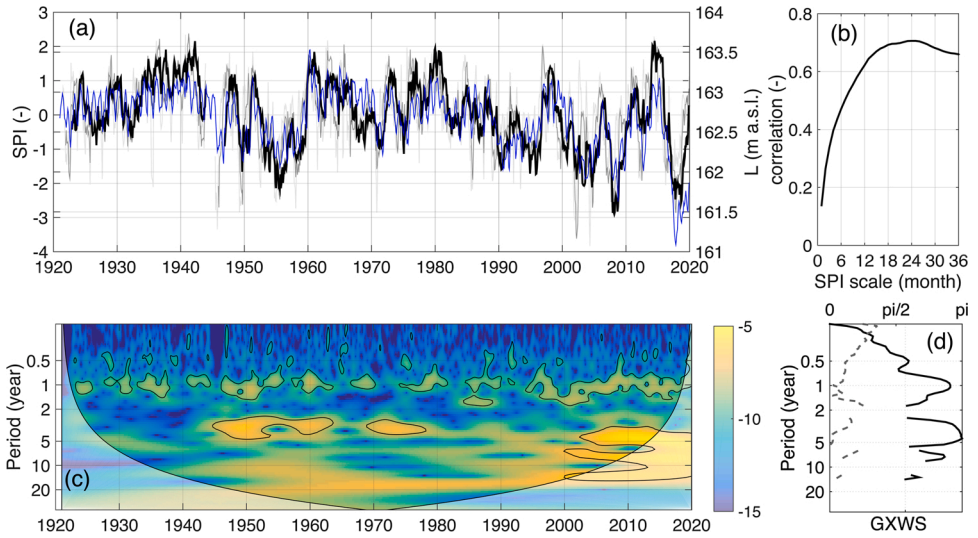

Fig. 3. Panel (a): Standardized Precipitation Index (SPI estimated at 6, 12 and 24 months (light grey, dark grey and thick black line respectively) over the precipitation time series (P). Monthly lake level (L) is reported on right axis as blue line. Panel (b): Pearson correlation coefficient between L and SPI at different time scales. Panel (c): Cross Wavelet Transforms among L and SPI24. Panel (d): associated Global Cross Wavelet Spectrum in Phase (dash line, upper x axis) and Amplitude (full line, lower x axis). (For interpretation of the references to colour in the Figure, the reader is referred to the web version of this article).

SPI1, SPI3, SPI6 and SPI12), consisting of multiscale runoff, shallow infiltration and evapotranspiration processes; (ii) variation in open water evaporation on the lake surface; (iii) variation in abstraction.

Fig. 4 highlights a sharp increase during the last decade in the long-term variation of L (Fig. 4a), SPI24 (Fig. 4b) and Q_{out} (Fig. 4c). In contrast to an earlier period (roughly from 1950 to 1965), in which only SPI24 and L were affected by increased variability, during the last decade increased of L variability (roughly from 0.3 to 0.6 m. a.s.l.) was accompanied by an increase in both SPI24 (from 0.7 to 1.2) and Q_{out} (from 0.3 to 0.5 $m^3\ s^{-1}$) variability.

The long-term variability of air temperature and open water evaporation from the lake are unfortunately not available. The impact of increasing mean temperature (+0.022 °C y^{-1} over the 1955–2019 period, Fig. 4f) on variation in L was considered in terms of the open water evaporation rate (Fig. 4e) and Q_{out} (Fig. 4f). The available dataset did not allow for investigation of the impact of increased

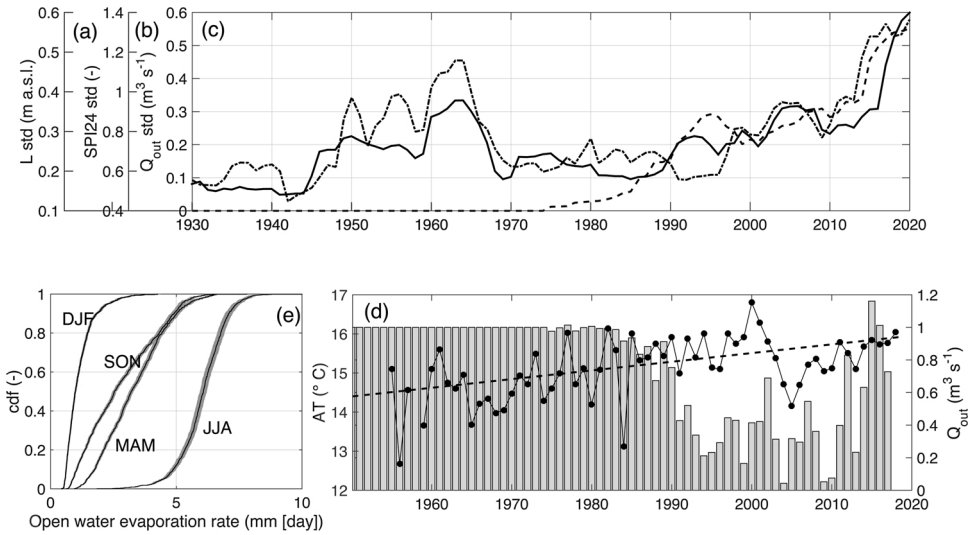

Fig. 4. Long-term variability of lake level: panel a) full line, L std, panel b) 24 month precipitation anomalies (dot line, SPI24 std, and panel c) mean abstraction (dashed line, Q_outˆ std). Mean annual air temperature (AT) and associated Sen's slope (0.022*** °C y-1) estimated over the 1955 – 2020 period, and mean annual withdraw Q_outˆ (panel d, black lines and grey bar on left and right axis, respectively). Seasonal cumulated density function of daily open water evaporation over the 2007-2017 period (panel e, black lines). DJF, MAM, JJA, and SON refer to winter, spring summer and autumn, respectively. Associated grey area has been obtained considering a range of [-1 + 1] °C for the air temperature compared to the 2007-2017 period.

temperature on vegetation or evapotranspiration and infiltration processes. The direct importance of monthly air temperature variability is assessed below in accordance with a machine learning approach (§ 5.1).

As presented in § 3.3, the possible impact of long-term temperature changes on evaporation from the lake was evaluated by means of the Penman equation, considering a mean variations of −1 °C and +1 °C with respect to the mean value of the 2007–2017 period (roughly representative of pristine and future conditions respectively), leaving the other meteorological parameters used to compute evaporation unchanged. As shown in Fig. 4f, the considered range of air temperatures did not affect the variability of open water surface evaporation as much as seasonal and inter-annual variability, much of which is driven by the wind speed (not shown). Similar results were also been reported in Rossi et al. (2019). The highest sensitivity to mean air temperature is observed in summer (JJA), during which the median difference between median daily evaporation rate under the two scenarios is 0.28 mm day^{-1} (i.e., less than 0.25 cm over 90 days). Finally, no correlation is observed between mean air temperature and the abstraction time series (Fig. 4f), at either the monthly or the annual scale ($r = 0.12$ and r=-0.03 respectively for the 1980–2019 period), indicating that the variability of Q_{out} observed since the early 1980s was not a response to air temperature.

5. Discussion

5.1. Relative impact of long-term precipitation and abstraction patterns on lake water level

Assessment of the relative contribution of the observed long-term precipitation and abstraction to the recent increase in L variations (Fig. 4a) is challenging considering the lack of long-term groundwater data (§ 2.1). A mass balance approach is not suitable when important terms are not available. A multi-regression approach, based on the assumption of a linear response to SPIs and abstraction variability, gives poor results and suffers from difficulties in both the normalization of abstraction time series data and high sensitivity to the baseline considered for calibration (not shown). In this section, we test the capacity of the *RF* Machine Learning approach for estimating the relative contribution of variation in precipitation and abstraction (Fig. 4b and c) to L variations (Fig. 4a). In order to adequately represent the hydrological processes influencing L variations across different time scales, we considered SPI1, SPI3, SPI6, SPI12 and SPI24 anomalies and AT as representative of the variability in the meteorological forcing, affecting hydrological processes ranging from superficial runoff and evapotranspiration to groundwater dynamics. The time series of Q_{out} is considered for abstraction. In order to take account of systematic seasonality, the month (indicated by an integer) is also considered. Indeed, as shown in Romano et al., 2017 and Romano et al. 2019, the impact of the precipitation anomalies, represented by SPIs, on the discharge, also depends on the months of the year. Finally, a random signal was added in order to monitor the permutation-based estimation of the variable's importance estimation.

The list of hyperparameters showing the best performance is given in Table 2. This parameter has been set to obtain the results presented below. Moreover, to monitor the influence of random selection of training and testing dataset on the overall results, each forest has been repeated 100 times, with a new random seed. Such solution, despite redundant to the *RF* approach, gives a further confidence on the performance and weighting results as it monitors the uncertainty introduced by the random selection of learning/training dataset.

The results of the *RF* simulations are presented in Fig. 5a, as the mean value of the 100 runs and associated standard deviation.

The overall influence of monthly mean air temperature variability on monthly L variability over the period 1955–2019, is shown in Fig. 5b. Each boxplot, sorted by its own median value, shows the drop-column importance values over the forests for each considered variable. SPI24, Q_{out} and month (month number) are the variables with greatest importance, followed by the SPI12, SPI3, SPI6 and T, which show very little importance. The importance of month number needs to be analyzed in combination with the associated time scale of the precipitation anomaly. Indeed, the precipitation anomaly at a given time scale can represent a very broad range of values in terms of the amount of water (thus having a different impact on L variation) due to seasonality (e.g. high precipitation in the summer months has a negligible impact on the lake water budget due to the strong evapotranspiration). In other words, the month number enables the model to interpret the SPIs with reference to the month. Finally, no significant difference ($p = 0.98$) is observed between the SPI1 and the random signal.

We also compared the performance of the learning and testing process with and without temperature data. This is somewhat similar to the drop-column importance, but even more straightforward. Whereas a slight (but significant, $p < 0.01$) improvement in r^2 (from 0.936 to 0.939) is observed for the learning performance when considering air temperature (Fig. 5c), no significant difference is observed in the testing performance (Fig. 5d, $p = 0.15$). These results indicate that the variability in monthly mean air temperature has a very small influence on monthly L variations. The systematic contribution of seasonality to evaporation rate is sufficiently described by the month number, confirming the preliminary results presented in Fig. 4.

Table 2
Random forest hyperparameters used in this study.

Hyper-parameter	Short description	Selected value
Number of estimators	Number of regression trees to be implemented	50
Maximum features	Maximum number of features/variable to be considered for splitting a node	All
Minimum samples split	Minimum number of samples required to split a node	8
Minimum sample leaf	Minimum number of samples required to be at leaf node.	1
Minimisation criterion	The function for measuring the quality of a split.	rmse

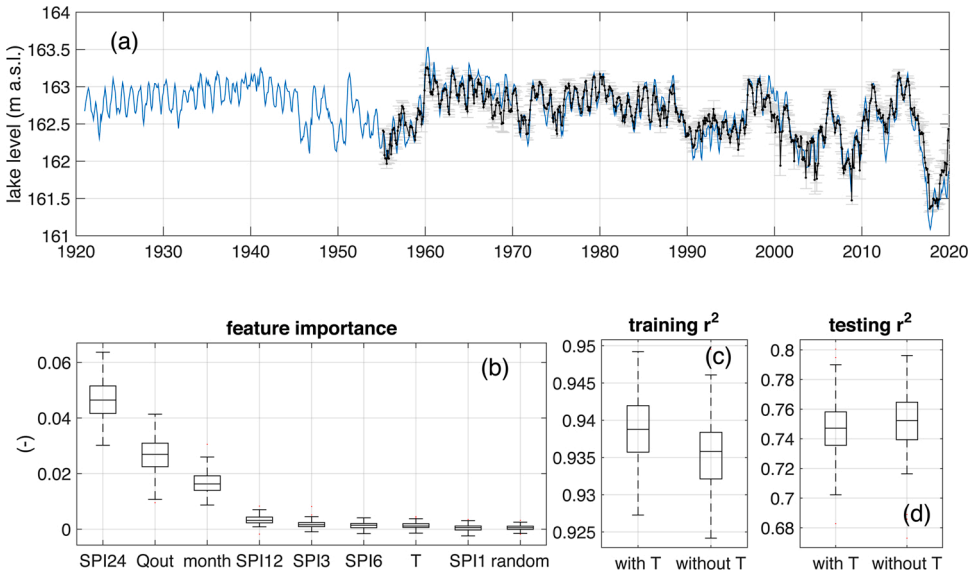

Fig. 5. Panel a: observed (blue line) and reproduced lake level (black line) and associated uncertainty to learning/training random selection (gray error bar). Panel b: relative feature importance and associated uncertainty to learning/training random selection. Panel c and d: overall performance as measure by r2, for training and testing dataset, respectively), considering or not T. (For interpretation of the references to colour in the Figure, the reader is referred to the web version of this article).

In the following, we remove SPI1 (as it makes the same contribution as the random signal) and T (as it is of very low importance, and has no significant impact on overall testing performances) from the simulations. This makes it possible to considering the whole 1921–2019 period.

The overall results obtained considering the whole period are shown in Fig. 6a (black line).

The training and testing median r^2 are 0.94 and 0.74, respectively (with a standard deviation associated with learning/training random selections of 0.0045 and 0.0020 respectively). The associated mean absolute errors are 0.08 and 0.15 m (a.s.l.), respectively.

We are interested in the role of the abstraction variability introduced after 1985 (Figs. 2c and 3 c). A straightforward way to measure the change in relative importance is to consider different learning periods, before and after 1985. The *L* time series obtained by means of pre and post 1985 learning periods are shwon in Fig. 6a. They present similar performances for both learning and testing ($r^2 = 0.90$ and 0.63, respectively for the 1921–1984 baseline and 0.93 and 0.72, respectively for the 1985–2019 baseline), but contrasting results can be observed for their forecast period (i.e., *L* reconstructed out from the learning/testing baseline). When learning

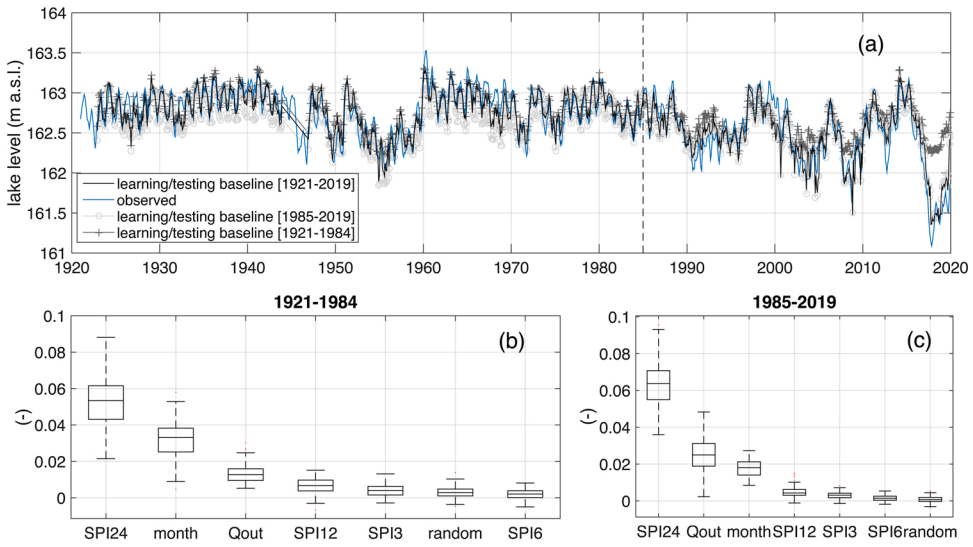

Fig. 6. Changes in feature importance between 1920-1994 and 1995-2019 periods. Panel a: observed and reconstructed lake level (m a.s.l.) over different learning/testing baselines (1921-2019, 1921-1984, 1985-2019). Panel b and c: relative feature importance for the learning/testing baseline 1921-1984 and 1985-2019, respectively.

based on the 1921–1984, the resulting reconstruction underestimates the sharp decrease in *L* during the second half of the 2000s and second half of the 2010s. This is due to the fact that the minimum level observed during the last decade had never been observed before (i.e., during the learning/testing baseline), and thus the model cannot reproduce them. Similarly, the model does not learn the impact of either the maximum abstraction or minimum SPI24 observed during the last decade and therefore may underestimate its relative importance. In contrast, when learning is based on 1985–2019, although the resulting reconstruction is able to reproduce the *L* variability (Fig. 4), it introduces a negative bias *before* 1985. Fig. 6b and c show the variables' importance estimated for the 1920–1984 and 1985–2019 periods respectively. Before 1985, the relative importance of abstraction is about 24 % of that of the long-term precipitation anomaly (SPI24). After 1985, it rises to 39 %.

5.2. Contribution of random forest

Generally, the performance of any modeling approach is evaluated with reference to its capacity for predicting and inferring data in order to test hypotheses, predicting values beyond the range in the training data, and developing possible scenarios (James et al., 2013).

The main contribution of *RF* in this case study derives from its ability to compensate for the lack of groundwater flow data. Indeed, it was able to predict the observed monthly *L* based on precipitation anomalies and abstraction time series alone, with a training and testing r^2 of 0.94 and 0.74, respectively (Fig. 6). This high predictive performance, in a context where the processes connecting predictors and predictands occurs over various time scales and overlaps each other, illustrates both ability of RF to overcome the multi-collinearity that can limit a multi-regressive approach over multi-scale SPIs (not shown) and to capture potential non-linear dependencies (De Andres 2006; Boulesteix et al., 2012). Moreover, it is important to stress that being non-parametric, RF can handle skewed and multi-modal data (as Q_{out}, not shown). In this regards, according to James et al. (2013), *RF* can be considered as the most flexible machine learning methods, with a wide range of applications in diverse areas (Tyralis et al., 2019).

Although predictive capacity is obviously a primary requirement, unlike the general class of data-driven models, *RF* also presents an interesting capacity for inference based on the variable importance metrics (e.g., Biau and Scornet, 2016). In this regards, in the present work, the main contribution of *RF* derives from its ability to infer the relative role of direct management and climate forcing (i.e., abstraction and temperature/precipitation respectively) in determining monthly *L* variations (Fig. 5). Specifically, the *RF* made it possible to highlight: a) the negligible role of temperature in the local lake dynamics; b) the major role played by the long-term precipitation variability in lake fluctuation over the last century of data; c) the increasing role of abstraction compared to long-term precipitation variability over the last two decades (from 24 % to 39 %, Fig. 6), by comparing the variable 's inferred importance over different baselines. According to James et al. (2013), *RF* is considered the second least interpretable of the machine learning algorithms (following the Support Vector Machines). However, the use of *RF* as a generic framework for predictive modelling, seems to be its main research function (Hengl et al., 2018).

In relation to *RF*'s ability to predict values beyond the range of the training period, we observed that the model failed to forecast the minimum *L* observed during the last two decades when the model was trained with reference to the 1921–1984 period (Fig. 6). This can be considered the main limitation of *RF* in non-stationarity contexts, i.e., that the algorithm cannot extrapolate beyond the training range, because the model cannot predict an event that has never been observed before (Hengl et al., 2018).

Moreover, *RF* cannot adequately model datasets with imbalanced data (i.e., datasets in which the number of observations of a response variable belonging to one class differs significantly compared to other classes) (Schubach et al., 2017). In other words, less can be learned from rare events than frequent ones. This underlying issue is partially addressed in the present study by testing the robustness of variable importance estimation to the random selection of learning/training datasets (Section 5.1). Nevertheless, the limitation remains if *RF* is used to provide scenarios, especially if the uniqueness of a given situation (e.g., the minimum L observed in 2017) does not allow the model to learn from similar conditions, thus preventing the use of *RF* for unusual management scenarios.

6. Conclusions

In this paper we presented new hydrological Insights into Lake Bracciano, a strategic water reservoir for the city of Rome. Specifically, this work clarified the relative impact of the two main drivers of change (climate and management) on water level fluctuations. We confirmed the marginal role of temperature, the increasing role of abstraction over the last two decades, and the major role played by increased variability of precipitation.

From a methodological point of view, the drivers' relative impact of drivers was estimated with the Random Forest machine learning approach. The results highlight the potential of the adopted technique in hydrological contexts, especially when data are incomplete, and present implications for the future management of abstraction.

We found that Random Forest is able to assess, in the absence of information on the connected groundwater dynamics, the relative importance of monthly abstraction, multi-scale precipitation anomalies and air temperature for the lake level variations. Specifically, in this case-study, our results indicate that: (i) air temperature and short-term precipitation anomalies can safely be ignored; (ii) long-term precipitation is the main driver of the lake level variability; (iii) the impact of abstraction on lake level oscillations has growin in the last two decades. We concluded by presenting the main limitations of the Random Forest approach in this context. Specifically, we pointed out that the model failed to predict beyond the range of the training period and thus was not able to predict an event that has never been observed before. In contrast, the Random Forest model's main contribution lies in inferring the role of management in a hydrological context complicated by the limited availability of data.

Author statement

Guyennon Nicolas: Conceptualization, Methodology, Software, Writing - Original Draft. **Salerno Franco:** Conceptualization, Investigation, Writing - Review & Editing, Visualization. **Rossi David:** Data curation, Writing - Review & Editing. **Rainaldi Martina:** Data curation. **Calizza Edoardo:** Writing - Review & Editing. **Romano Emanuele:** Formal analysis, Investigation, Writing - Review & Editing, Supervision.

Declaration of Competing Interest

The authors report no declarations of interest.

Acknowledgements

The authors are grateful to the Servizio Meteorologico dell'Aeronautica Militare and the Civil Protection Agency of Lazio region for providing the climate data set of Bracciano, to ACEA-ATO2 for providing abstraction data and to the Park Authority of Bracciano-Martignano for providing lake water level. We thank the reviewers and editor for their constructive comments and George Metcalf for revising the English text.

This research did not receive any specific grant from funding agencies in the public, commercial, or not-for-profit sectors.

Appendix A. Supplementary data

Supplementary material related to this article can be found, in the online version, at doi:https://doi.org/10.1016/j.ejrh.2021.100880.

References

Abrahart, R.J., Anctil, F., Coulibaly, P., Dawson, C.W., Mount, N.J., See, L.M., Shamseldin, A.Y., Solomatine, D.P., Toth, E., Wilby, R.L., 2012. Two decades of anarchy? Emerging themes and outstanding challenges for neural network river forecasting. Prog. Phys. Geogr. Earth Environ. 36, 480–513. https://doi.org/10.1177/0309133312444943.

ACEA, 2015. Sustainability Report. https://www.gruppo.acea.it/content/dam/acea-corporate/acea-foundation/pdf/en/company/sustainability/SustainabilityReport/sustainability-report-2015-acea-group.pdf.

Aguilera, P.A., Fernández, A., Fernández, R., Rumí, R., Salmerón, A., 2011. Bayesian networks in environmental modelling. Environ. Model. Softw. 26, 1376–1388. https://doi.org/10.1016/j.envsoft.2011.06.004.

Ardabili, S., Mosavi, A., Dehghani, M., Várkonyi-Kóczy, A.R., 2019. Deep learning and machine learning in hydrological processes climate change and earth systems a systematic review. September. In: International Conference on Global Research and Education. Springer, Cham, pp. 52–62.

Armenia, S., Bellomo, D., Medaglia, C.M., Nonino, F., pompei, A., 2019. Water resource management through systemic approach: the case of Lake Bracciano. J. Simul. https://doi.org/10.1080/17477778.2019.1664266.

Azzella, M.M., 2014. Italian Volcanic lakes: a diversity hotspot and refuge for European charophytes. J. Limnol. 73 (3), 502–510. https://doi.org/10.4081/jlimnol.2014.950.

Azzella, M.M., Bresciani, M., Nizzoli, D., Bolpagni, R., 2017. Aquatic vegetation in deep lakes: macrophyte co-occurrence patterns and environmental determinants. J. Limnol. 76 (S1), 97–108. https://doi.org/10.4081/jlimnol.2017.1687.

Baccetti, N., Bellucci, V., Bernabei, S., Bianco, P., Braca, G., Bussettini, M., Cascone, C., Ciccarese, L., D'Antoni, S., Grignetti, A., Lastoria, B., Mandrone, S., Mariani, S., Silli, V., Venturelli, S., 2017. - Analisi E Valutazione Dello Stato Ambientale Del Lago Di Bracciano Riferito All'estate 2017. Rapporto ISPRA, 18 Ottobre 2017, 56pp. (in Italian).

Biau, G., Scornet, E., 2016. A Random Forest guided tour. Test 25 (2), 197–227. https://doi.org/10.1007/s11749-016-0481-7.

Blöschl, G., 2001. Scaling in hydrology. Hydrol. Process. 15, 709–711. https://doi.org/10.1002/hyp.432.

Boulesteix, A.L., Janitza, S., Kruppa, J., König, I.R., 2012. Overview of Random Forest methodology and practical guidance with emphasis on computational biology and bioinformatics. Wiley Interdiscip. Rev. Data Min. Knowl. Discov. 2, 493–507. https://doi.org/10.1002/widm.1072.

Bowden, G.J., Dandy, G.C., Maier, H.R., 2005. Input determination for neural network models in water resources applications. Part 1—background and methodology. J. Hydrol. 301, 75–92. https://doi.org/10.1016/j.jhydrol.2004.06.021.

Breiman, L., 1996. Bagging predictors. Mach. Learn. 24 (2), 123–140. https://doi.org/10.1007/BF00058655.

Breiman, L., 2001. Random forests. Mach. Learn. 45 (1), 5–32. https://doi.org/10.1023/A:1010933404324.

Buitinck, L., Louppe, G., Blondel, M., Pedregosa, F., Mueller, A., Grisel, O., et al., 2013. API Design for Machine Learning Software: Experiences from the Scikit-learn Project. arXiv Preprint. arXiv:1309.0238..

Calizza, E., Rossi, L., Careddu, G., Caputi, S.S., Costantini, M.L., 2021. A novel approach to quantifying trophic interaction strengths and impact of invasive species in food webs. Biol. Inv. 1–15. https://doi.org/10.1007/s10530-021-02490-y in press.

Carpenter, S.R., Lodge, D.M., 1986. Effects of submersed macrophytes on ecosystem processes. Aquat. Bot. 26, 341–370. https://doi.org/10.1016/0304-3770(86)90031-8.

Cordiano, G., Barricelli, A., Insolera, E., et al., 2014. - Villae and unusual lateres stamps in the area of Bracciano Lake | Villae e bolli inediti su lateres nel comprensorio del Lago di Bracciano. ErgaLogoi 2 (1), 103–154. https://doi.org/10.7358/erga-2014-001-cord, 2014.

Costantini, M.L., Carlino, P., Calizza, E., Careddu, G., Cicala, D., Sporta Caputi, S., Fiorentino, F., Rossi, L., 2018. The role of alien fish (the centrarchid Micropterus salmoides) in lake food webs highlighted by stable isotope analysis. Freshw. Biol. 63 (9), 1130–1142. https://doi.org/10.1111/fwb.13122.

Dawson, C.W., Wilby, R.L., 2001. Hydrological modelling using artificial neural networks. Prog. Phys. Geogr. 25 (1), 80–108. https://doi.org/10.1177/030913330102500104.

De Rita, D., Di Filippo, M., Rosa, C., 1996. - Structural evolution of the Bracciano volcano-tectonic depression, Sabatini Volcanic District. Italy. Geol. Soc. Spec. Publ. 110, 225–236. https://doi.org/10.1144/GSL.SP.1996.110.01.17, 1996.

Dee, D.P., Uppala, S.M., Simmons, A.J., Berrisford, P., Poli, P., Kobayashi, S., Andrae, U., Balmaseda, M.A., Balsamo, G., Bauer, P., Bechtold, A.C.M., Van de Berg, L., Bidlot, J., Bromann, N., Delsol, C., Dragani, R., Fuentes, M., Geer, A.J., Haimberger, L., Healy, S.B., Hersbach, H., Hòlm, E.V., Isaksen, P., Kallberg, P., Kohler, M.,

Matricardi, M., McNally, A.P., Monge-Sanz, B.M., Morcrette, J.J., Park, K., Peubey, C., De Rosnay, P., Tavolato, C., Thépat, J.N., Vitart, F., 2011. The ERA-Interim reanalysis: configuration and performance of the data assimilation system. Q. J. R. Meteorol. Soc. 137 (656), 553–597. https://doi.org/10.1002/qj.828.

Di Filippo, M., Ruspandini, T., Toro, B., 1998. Geophysical contribution to the study of Bracciano Lake. Quat. Int. 47/48, 29–34. https://doi.org/10.1016/S1040-6182(97)00067-0, 1998.

Díaz-Uriarte, R., De Andres, S.A., 2006. Gene selection and classification of microarray data using Random Forest. BMC Bioinformatics 7 (1), 3. https://doi.org/10.1186/1471-2105-7-3.

Galloway, J.N., Aber, J.D., Erisman, J.W., Seitzinger, S.P., Howarth, R.W., Cowling, E.B., Cosby, B.J., 2003. The nitrogen cascade. Bioscience 53 (4), 341–356. https://doi.org/10.1641/0006-3568(2003)053[0341:TNC]2.0.CO;2.

Grinsted, A., Moore, J.C., Jevrejeva, S., 2004. Application of the cross wavelet transform and wavelet coherence to geophysical time series. Nonlinear Process. Geophys. Discuss. 11, 561–566. https://doi.org/10.5194/npg-11-561-2004.

Guyennon, N., Romano, E., Portoghese, I., Salerno, F., Calmanti, S., Petrangeli, A.B., Tartari, G., Copetti, D., 2013. Benefits from using combined dynamical-statistical downscaling approaches–lessons from a case study in the Mediterranean region. Hydrol. Earth Syst. Sci. 17 (2), 705–720. https://doi.org/10.5194/hess-17-705-2013.

Guyennon, N., Valerio, G., Salerno, F., Pilotti, M., Tartari, G., Copetti, D., 2014. Internal wave weather heterogeneity in a deep multi-basin subalpine lake resulting from wavelet transform and numerical analysis. Adv. Water Resour. 71, 149–161. https://doi.org/10.1016/j.advwatres.2014.06.013.

Guyennon, N., Romano, E., Portoghese, I., 2016. Long-term climate sensitivity of an integrated water supply system: the role of irrigation. Sci. Total Environ. 565, 68–81. https://doi.org/10.1016/j.scitotenv.2016.04.157.

Guyennon, N., Salerno, F., Portoghese, I., Romano, E., 2017. Climate change adaptation in a Mediterranean semi-arid catchment: testing managed aquifer recharge and increased surface reservoir capacity. Water 9 (9), 689. https://doi.org/10.3390/w9090689.

Hengl, T., Nussbaum, M., Wright, M.N., Heuvelink, G.B., Gräler, B., 2018. Random forest as a generic framework for predictive modeling of spatial and spatio-temporal variables. Peer J 6, e5518. https://doi.org/10.7717/peerj.5518.

James, G., Witten, D., Hastie, T., Tibshirani, R., 2013. An Introduction to Statistical Learning, vol. 112. New York: springer, p. 18.

Kendall, M.G., 1948. Rank Correlation Methods.

Kendall, C., Elliot, E.M., Wankel, S.D., 2010. Tracing anthropogenic inputs of nitrogen to ecosystems. Stable Isotopes in Ecology and Environmental Science. Blackwell Publishing, pp. 375–449. https://doi.org/10.1002/9780470691854.ch12.

Liaw, A., Wiener, M., 2002. Classification and regression by random Forest. R news 2 (3), 18–22.

Linacre, E.T., 1993. Data-sparse estimation of lake evaporation, using a simplified Penman equation. Agric. For. Meteorol. 64 (3–4), 237–256. https://doi.org/10.1016/0168-1923(93)90031-C.

Liu, Y., Liang, X.S., Weisberg, R.H., 2007. Rectification of the bias in the wavelet power spectrum. J Atmos Ocean Technol 24, 2093–2102. https://doi.org/10.1175/2007JTECHO511.1.

Loh, W.Y., 2011. Classification and regression trees. Wiley Interdiscip. Rev. Data Min. Knowl. Discov. 1 (1), 14–23. https://doi.org/10.1002/widm.8.

Malinverno, A., Ryan, W.B.F., 1986. – Extension in the Tyrrhenian sea and shortening in the Appennines as result of arc migration driven by sinking of the lithosphere. TECTONICS 5 (2 April), 227–245. https://doi.org/10.1029/TC005i002p00227, 1986.

McKee, T.B., Doeskin, N.J., Kieist, J., 1993. The relationship of drought frequency and duration to time scales. Proc. 8th Conf. on Applied Climatology, January 17-22, 1993, American Meteorological Society, Boston, Massachusetts 179–184.

McKee, T.B., Doeskin, N.J., Kieist, J., 1995. Drought monitoring with multiple time scales. Proc. 9th Conf. on Applied Climatology, January 15-20, 1995, American Meteorological Society, Boston, Massachusetts 233–236.

Naghibi, S.A., Dolatkordestani, M., Rezaei, A., et al., 2019. Application of rotation forest with decision trees as base classifier and a novel ensemble model in spatial modeling of groundwater potential. Environ. Monit. Assess. 191, 248. https://doi.org/10.1007/s10661-019-7362-y.

Nalbantis, I., Tsakiris, G., 2009. Assessment of hydrological drought revisited. Water Resour. Manage. 23 (5), 881–897. https://doi.org/10.1007/s11269-008-9305-1.

Nicolosi, I., Caracciolo, F.A., Pignatelli, A., Chiappini, M., 2019. Imaging the Bracciano caldera system by aeromagnetic data inversion (Sabatini Volcanic District, Central Italy). J. Volcanol. Geotherm. Res. 388, 106680. https://doi.org/10.1016/j.jvolgeores.2019.106680.

Ostroumov, S.A., 2017. Water quality and conditioning in natural ecosystems: biomachinery theory of self-purification of water. Russ. J. Gen. Chem. 87 (13), 3199–3204. https://doi.org/10.1134/S107036321713014X.

Paper, D., 2020. Scikit-learn classifier tuning from complex training sets. Hands-on Scikit-learn for Machine Learning Applications: Data Science Fundamentals with Python, pp. 165–188.

Parr, T., Turgutlu, K., Csiszar, C., Howard, J., 2018. Beware Default Random Forest Importances. https://explained.ai/rf-importance/index.html.

Pedregosa, F., Varoquaux, G., Gramfort, A., Michel, V., Thirion, B., Grisel, O., Blondel, M., Prettenhofer, P., Weiss, R., Dubourg, V., Vanderplas, J., Passos, A., Cournapeau, D., Brucher, M., Perrot, M., Duchesnay, E., 2011. Scikit-learn: machine learning in Python. J. Mach. Learn. Res. 12, 2825-2.

Penman, H.L., 1948. Natural evaporation from open water, bare soil and grass Proc. Roy. Soc. Lond. A 193, 120–146. https://doi.org/10.1098/rspa.1948.0037.

Penman, H.L., 1956. Evaporation: an introductory survey Neth. J. Agric. Sci. 4, 9–29. https://doi.org/10.18174/njas.v4i1.17768.

Phan, T.D., Smart, J.C.R., Capon, S.J., Hadwen, W.L., Sahin, O., 2016. Applications of Bayesian belief networks in water resource management: a systematic review. Environ. Model. Softw. 85, 98–111. https://doi.org/10.1016/j.envsoft.2016.08.006.

Raghavendra, S., Deka, P.C., 2014. Support vector machine applications in the field of hydrology: a review. Appl. Soft Comput. 19, 372–386. https://doi.org/10.1016/j.asoc.2014.02.002.

Romano, E., Giudici, M., 2007. Experimental and modeling study of the soil-atmosphere interaction and unsaturated water flow to estimate the recharge of a phreatic aquifer. J. Hydrol. Eng. 12 (6), 573–584. https://doi.org/10.1061/(ASCE)1084-0699(2007)12:6(573).

Romano, E., Giudici, M., 2009. On the use of meteorological data to assess the evaporation from a bare soil. J. Hydrol. 372, 30–40. https://doi.org/10.1016/j.jhydrol.2009.04.003.

Romano, E., Preziosi, E., 2013. Precipitation pattern analysis in the Tiber River basin (central Italy) using standardized indices. Int. J. Climatol. 33 (7), 1781–1792. https://doi.org/10.1002/joc.3549.

Romano, E., Del Bon, A., Petrangeli, A.B., Preziosi, E., 2013. Generating synthetic time series of springs discharge in relation to standardized precipitation indices. Case study in Central Italy. J. Hydrol. 507, 86–99. https://doi.org/10.1016/j.jhydrol.2013.10.020.

Romano, E., Guyennon, N., Del Bon, A., Petrangeli, A.B., Preziosi, E., 2017. Robust method to quantify the risk of shortage for water supply systems. J. Hydrol. Eng. 22 (8), 04017021. https://doi.org/10.1061/(ASCE)HE.1943-5584.0001540.

Romano, E., Guyennon, N., Duro, A., Giordano, R., Petrangeli, A.B., Portoghese, I., Salerno, F., 2018. A stakeholder oriented modelling framework for the early detection of shortage in water supply systems. Water 10 (7262). https://doi.org/10.3390/w10060762.

Rossi, L., Costantini, M.L., Carlino, P., Di Lascio, A., Rossi, D., 2010. Autochthonous and allochthonous plant contributions to coastal benthic detritus deposits: a dual-stable isotope study in a volcanic lake. Aquatic Sci. 72 (2), 227–236. https://doi.org/10.1007/s00027-009-0125-z.

Rossi, D., Romano, E., Guyennon, N., Rainaldi, M., Ghergo, S., Mecali, A., Parrone, D., Taviani, S., Scala, A., Perugini, E., 2019. The present state of Lake Bracciano: Hope and despair. Rendiconti Lincei. Sci. Fisiche E Naturali 30 (1), 83–91. https://doi.org/10.1007/s12210-018-0733-4.

Schubach, M., Re, M., Robinson, P.N., Valentini, G., 2017. Imbalance-aware machine learning for predicting rare and common disease-associated non-coding variants. Sci. Rep. 7 (1), 1–12. https://doi.org/10.1038/s41598-017-03011-5.

Sen, P.K., 1968. Estimates of the regression coefficient based on Kendall's tau. J. Am. Stat. Assoc. 63, 1379–1389.

Shuttleworth, D.R., 1993. In: Maidment (Ed.), Evaporation. McGraw-Hill, New York, pp. 4.1–4.53. Chapter 4).

Sivapalan, M., 2003. Process complexity at hillslope scale, process simplicity at the watershed scale: is there a connection? Hydrol. Process. 17, 1037–1041. https://doi.org/10.1002/hyp.5109.

Strobl, C., Boulesteix, A.L., Kneib, T., Augustin, T., Zeileis, A., 2008. Conditional variable importance for random forests. BMC Bioinformatics 9 (1), 307. https://doi.org/10.1186/1471-2105-9-307.

Strobl, C., Zeileis, A., 2008. Danger: High power!–exploring the statistical properties of a test for random Forest variable importance. In: Brito, P. (Ed.), COMPSTAT 2008 –Proceedings in Computational Statistics, Volume II, 59–66. Physica Verlag,Heidelberg, Germany. ISBN 978-3-7908-2083-2086.

Taviani, S., Henriksen, H.J., 2015. The application of a groundwater/surface-water model to test the vulnerability of Bracciano Lake (near Rome, Italy) to climatic and water-use stresses. Hydrogeol. J. 23, 1481–1498. https://doi.org/10.1007/s10040-015-1271-0.

Thakuri, S., Dahal, S., Shrestha, D., Guyennon, N., Romano, E., Colombo, N., Salerno, F., 2019. Elevation-dependent warming of maximum air temperature in Nepal during 1976–2015. Atmos. Res. 228, 261–269. https://doi.org/10.1016/j.atmosres.2019.06.006.

Tyralis, H., Papacharalampous, G., Langousis, A., 2019. A brief review of random forests for water scientists and practitioners and their recent history in water resources. Water 11, 910. https://doi.org/10.3390/w11050910.

World Meteorological Organization, 2012. Standardized Precipitation Index. User Guide. WMO-No. 1090, 24 pp. http://www.wamis.org/agm/pubs/SPI/WMO_1090_EN.pdf).

Ziegler, A., König, I.R., 2014. Mining data with Random Forests: current options for real-world applications. Wiley Interdiscip. Rev. Data Min. Knowl. Discov. 4, 55–63. https://doi.org/10.1002/widm.1114.